

5.3. Palmer Station, Antarctica

Palmer Station, established by the United States in 1965, is located on Anvers Island at 64°46' S, 64°03' W, slightly outside the Antarctic Circle. Palmer Station is manned year-around and has diverse flora and fauna. Various experiments, mostly relating to biological sciences, take advantage of the laboratory and field facilities. Palmer is also part of the Long Term Ecological Research (LTER) program. The population in winter is eight to twelve with a maximum of 32 in summer. Access is by icebreaker or ice-strengthened vessel.

The UV Spectroradiometer system at Palmer Station was originally installed in the roof of the vestibule of the Clean Air Building and was relocated to Building T-5 in March 1993. As at other sites, the data are originally recorded onto both a 120-MB, removable hard disk media and a hard disk drive internal to the system control computer. Data archiving is automated. The system control computer, utilizing the Windows NT® operating system and the Palmer Station Local Area Network (LAN), is setup as a File Transfer Protocol (FTP) server. This allows for data to be directly transferred by BSI staff from the system control computer via the Internet gateway at Palmer, limited only by satellite windows. Files can also be transferred as e-mail attachments, or FTP'd by the operator.

These archived files are transmitted via the ATS-3 or INMARSAT satellites. The location of Palmer makes it possible to transmit daily to the ATS-VAX or another SPAN node and then to Biospherical Instruments Inc. The T-5 Building is not continuously manned, but is visited regularly, usually every day. The system is operated by ASA personnel that have been trained by BSI. Palmer Station is normally accessible at intervals of approximately once per month.



Figure 5.3.1. Palmer Station, Antarctica (USA)

Table 5.3.1 Palmer Station (T-5): bearings of obstructions to the instrument's field-of-view.

Object Name	Bearing (degrees)	Elevation (degrees)
Glacier	310°-0°	3° - 4.5°
Glacier	0°-110°	4.5° - 5°
Air Vent	80°	7°
Glacier	110°-135°	4.5° - 1°
Ocean	135°-310°	0°
Distant mountain	152°	3°
Ladder to roof box	277°	15°
Lichtfield Island	283°	0.5°

Notes: Sightings made by T.B. Lucas of BSI using Brunton pocket transit during the March 1990 site visit. Instrument is at 13 meters above sea level.

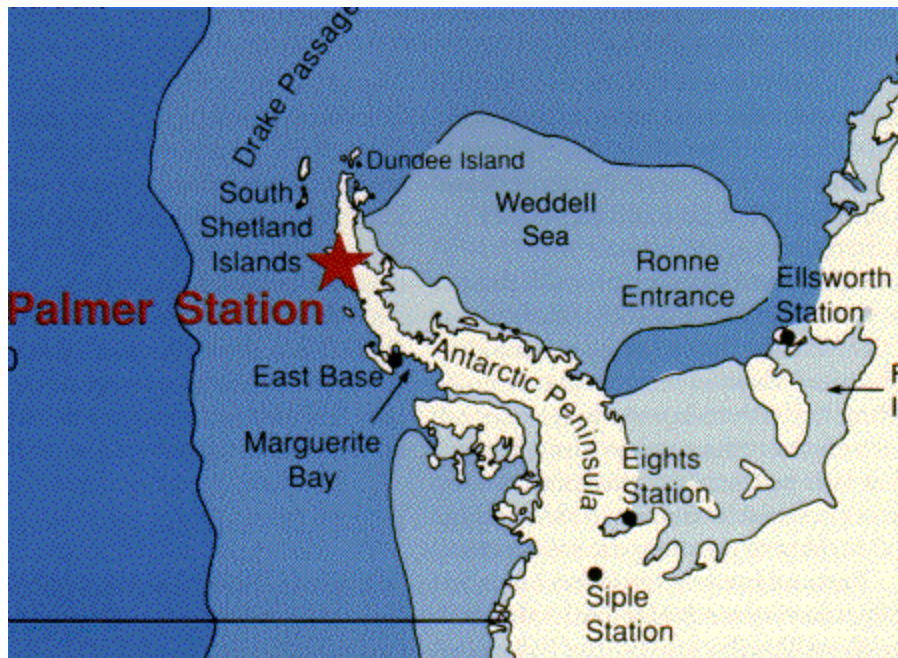


Figure 5.3.2. Palmer Station (map courtesy of USAP).

From the initial installation of the instrument on 5/19/88 in the original configuration (Version A) until September 1988, data collected were compromised by carbon buildup in the integrating sphere and by distortions in the dome protecting the entrance to the sphere. Starting 9/22/88, these components were replaced and the system was upgraded to Version B. The system was operated for the rest of the 1988 season by Dan Lubin (results were published in Lubin, 1989; Lubin et al., 1989, 1990, 1991, 1992).

January 1989 saw a considerable loss of data due to host computer failure. Operation was also marginal during the austral spring of 1989 as a result of temperature instabilities and design flaws in the monochromators. Starting 11/1/89, some data were compromised due to shutter problems. Finally, the system was taken off-line between 1/22/90 and 3/14/90 while a new monochromator was installed. Between 3/14/90 and the end of season 3/22/91 minor gaps existed in the data. Instabilities in the monochromator contributed more degradation in the Version B system performance than was expected. Therefore, the instrument was partially upgraded to a Version C system in May 1991, with completion of the upgrade in August 1991. Since the site visit on 8/22/91, the system has performed with excellent stability and minimal data loss.

At the site visit in March 1993, the instrument was moved from the Clean Air/ULF building to T-5. This move was to facilitate improved instrument operation, serviceability, and thermal management. With the exception of annual site visit periods, the system has operated continuously since. The system has received minor system upgrades over the years.

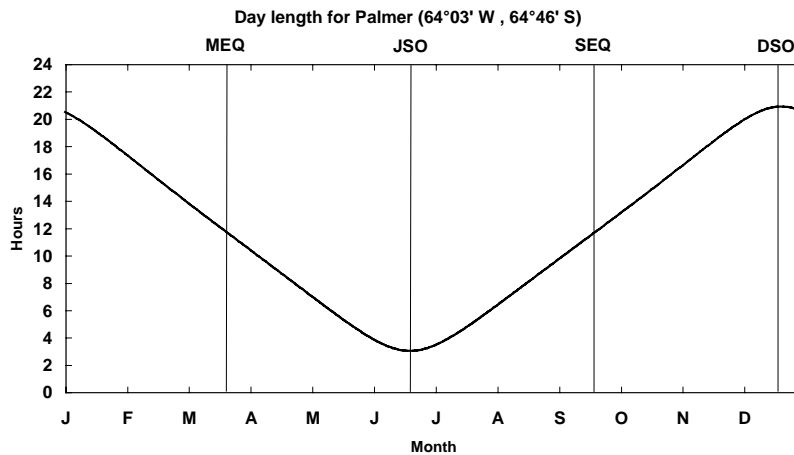


Figure 5.3.3. Day length for Palmer Station. (MEQ = March equinox, JSO = June solstice, SEQ = September equinox, DSO = December solstice.)

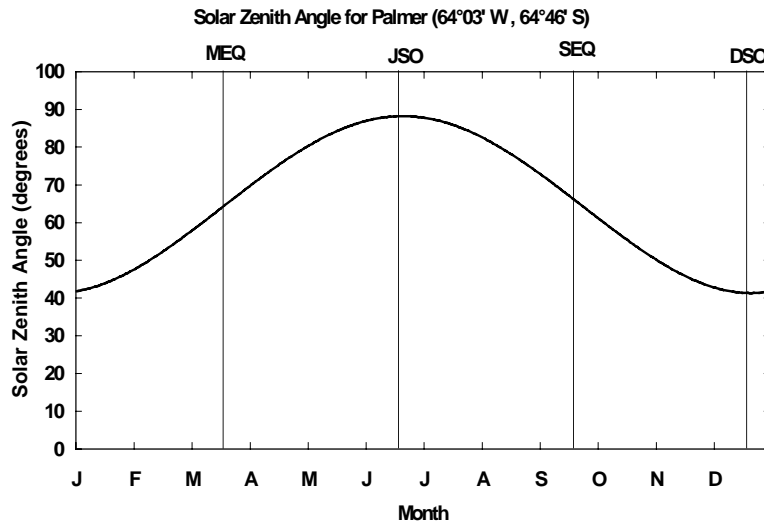


Figure 5.3.4. Noontime solar zenith angle during the year at Palmer.

5.3.1. Weather Observations

Weather observations for Palmer Station (WMO station number 89061) were obtained from the National Climatic Data Center (NCDC). The data are in a format described in Appendix A7 of this report. The data readings for Palmer are sporadic, ranging from daily to ten-day increments, and not available beyond October 1997, at the time of the CD-ROM pressing. The file, PALMER.CSV, can be found in the \WEATHER subdirectory on the CD-ROM 7.0.a.

5.3.2. Ozone Observations

Table 5.3.2. TOMS ozone averages and minima for Palmer, September 1 – December 31.

Year	TOMS												TOVS			
	Nimbus 7			Meteor 3			Adeos			Earth Probe			Avg	Min	Date	
	Avg	Min	Date	Avg	Min	Date	Avg	Min	Date	Avg	Min	Date				
1988	296.9	200	10/14/88													
1989	286.3	164	10/15/89													
1990	259.2	164	10/13/90													
1991	280.3	140	10/8/91	276.5	149	10/8/91										
1992	270.0	131	10/6/92	270.4	144	10/6/92										
1993				248.3	136	9/28/93										
1994				214.8	132	9/25/94							251.6	158	10/2/94	
1995													261.5	172	10/14/95	
1996							254.0	155	9/12/96	251.5	147	9/17/96	254.2	183	10/18/96	
1997										261.8	148.1	10/5/97				
1998										264.1	124.1	10/1/98				

Note: 1996 TOMS/Adeos data is only partially available; actual data starts on 9/11/96. 1998 TOMS/Earth Probe data is not available after 12/12/98. The average was therefore calculated from the period 9/1/98 – 12/12/98. The ozone value of 124.1 DU on 10/1/98 was the lowest ozone column ever measured at Palmer.

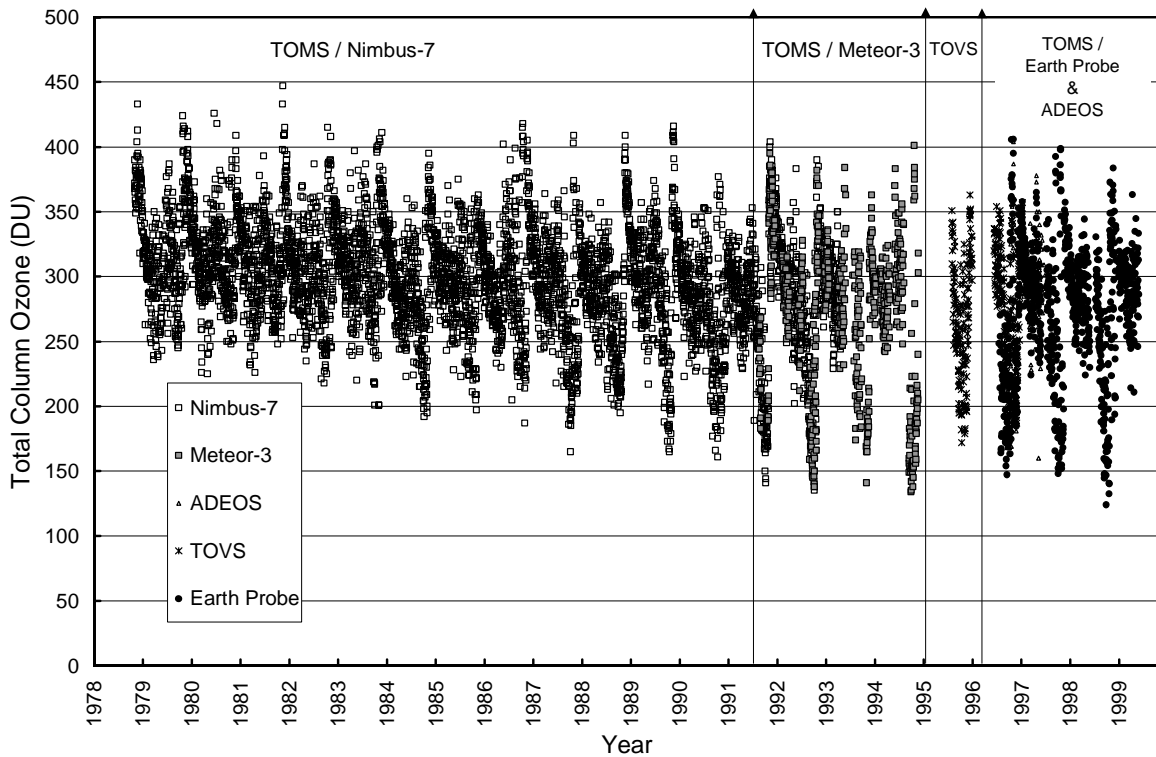


Figure 5.3.5 Time record of total column ozone from TOMS and TOVS data at Palmer Station.

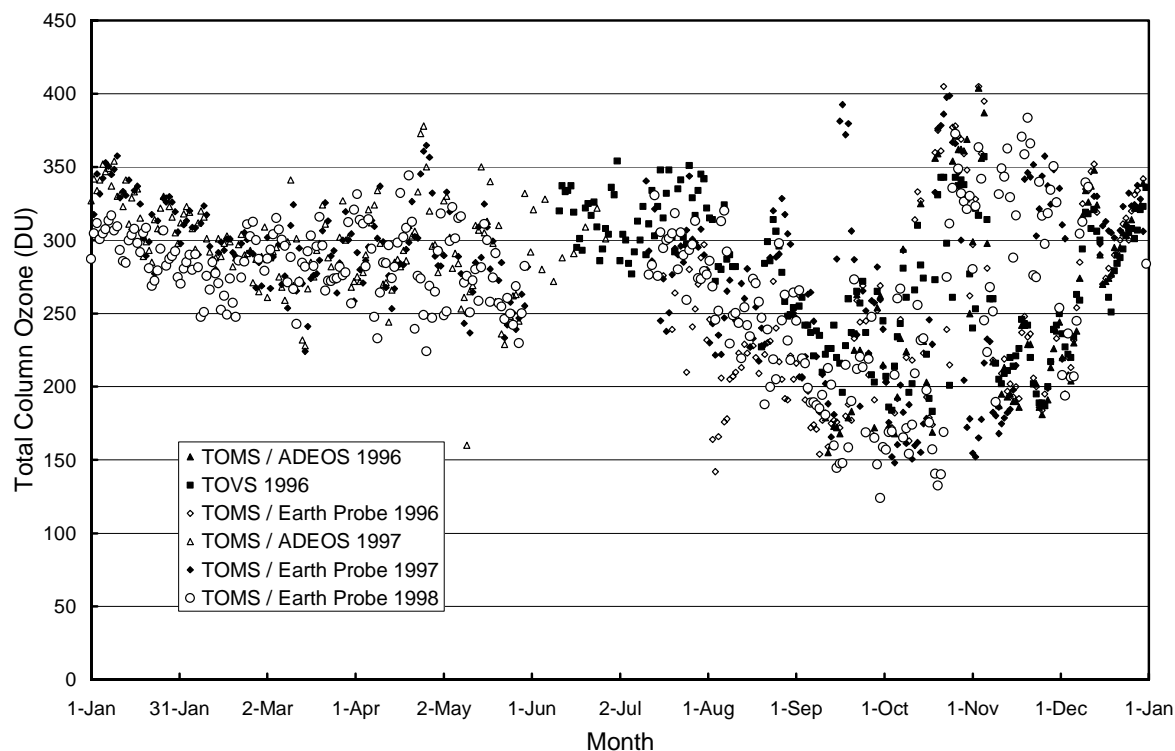


Figure 5.3.6. Yearly variation of ozone at Palmer. (Differences between satellites are discussed in Appendix A6. "Ozone Data.") In recent years, including 1997 and 1998, ozone depletion has been observed fairly early in the season; typically known to occur in October.

5.3.3. Palmer Station 4/10/97 - 4/5/98

The 1997/98 season at Palmer Station is defined as the time between the site visits, 4/10/97 – 4/18/97 and 3/26/98 – 4/5/98. The season opening and closing calibrations were performed on 4/16/97 and 3/26/98, respectively. Solar data is available for the period 4/19/97 – 3/25/98. During this time, the system operated normally. However, in the first three months of the season the response lamp showed a drift of about 10%. Calibrations with the 200-Watt standard lamps demonstrated that the system itself was very stable. During the problematic period, solar measurements had to be calibrated in a fashion differing from the normal procedure, as described below. Careful analysis showed that the drifting response lamp did not affect the accuracy of solar data.

5.3.3.1. Stability in the Wavelength Domain

As for the other sites, wavelength stability of the system was monitored with the internal Mercury lamp. Information from the daily wavelength scans was used to homogenize the data set by correcting day-to-day fluctuations of the wavelength offset. After this step, there may still be a deviation from the correct wavelength scale but this bias should ideally be the same for all days. Figure 5.3.7 shows the differences in the wavelength offset of the 296.73 nm Mercury line between two consecutive wavelength scans. In total, 336 scans have been evaluated. For 90% of the days, the change in offset is smaller than ± 0.025 nm; for 99% of the days the shift is smaller than ± 0.075 nm. The offset-difference is only larger than ± 0.1 nm for 4 scans (1.2%), see Table 5.3.3.

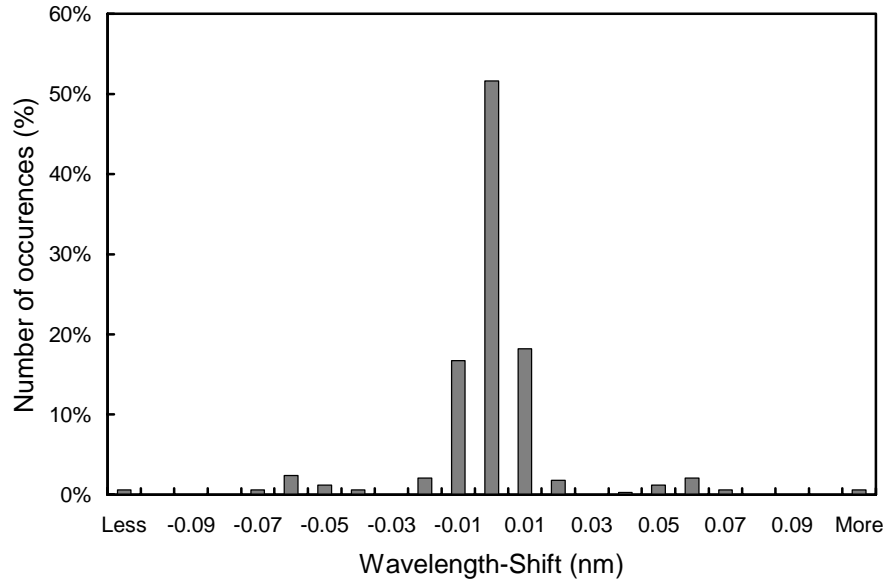


Figure 5.3.7. Differences in the measured position of the 296.72 nm Mercury line between consecutive wavelength scans. The x-labels give the center wavelength shift for each column. Thus the 0-nm histogram column covers the range -0.005 to +0.005 nm. “Less” means shifts smaller than -0.105 nm; “more” means shifts larger than 0.105 nm.

Table 5.3.3. Worst-case wavelength differences between consecutive scans.

First Wavelength File	Second Wavelength File	First Date	Second Date	Wavelength shift Second-First	Cause
BM970330.109	BM970300.110	4/19/97	4/20/97	-0.182	First scan after site visit
BM970330.203	BM970330.204	7/22/97	7/23/97	0.243	System malfunction
BM970330.204	BM970330.205	7/23/97	7/24/97	-0.185	System malfunction
BM980330.023	BM980330.024	1/23/98	1/24/98	0.179	Wavelength position manually adjusted

After the data was corrected for day-to-day wavelength fluctuations, the wavelength-dependent bias between this homogenized data set and the correct wavelength scale was determined with the Fraunhofer-correlation method, as described in Section 3. The thick line in Figure 5.3.8 shows the resulting correction function that was applied to the Volume 7 Palmer data. The function clearly depends on wavelength. This is caused by non-linearities in the monochromator drive. In order to demonstrate the difference between the result of the new Fraunhofer-correlation method and the method that was historically applied, Figure 5.3.8 also includes a correction function that was calculated with the “old” method, i.e., the function is based on internal wavelength scans only. The average difference between both approaches is 0.111 nm. As explained in Section 3, this bias is caused by the different light paths for internal wavelength scans and solar measurements.

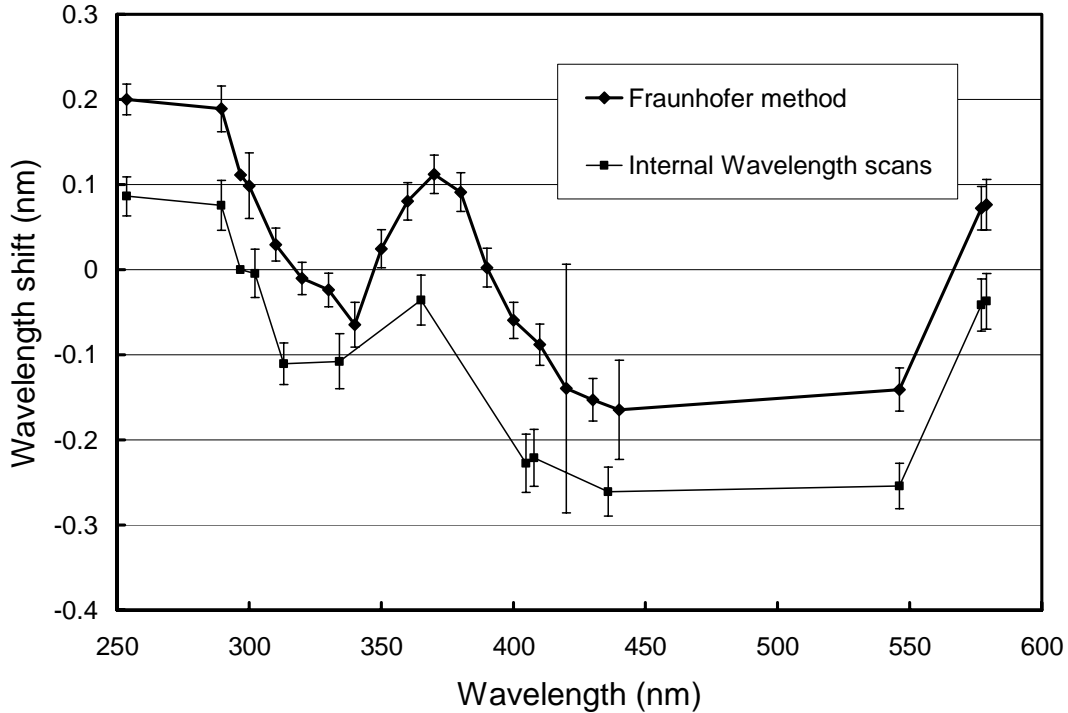


Figure 5.3.8. Functions expressing the monochromator non-linearity for Palmer. Thick line: Function calculated with the Fraunhofer-correlation method. This function was applied to correct the Palmer Volume 7 data. Thin line: Function calculated with the method that was historically applied. The offset between both methods is 0.111 nm. Both functions represent average wavelength shifts for the 1997/98 season. The error bars give the 1σ standard deviation variation of the wavelength shifts of individual days. The larger error bar at 420 nm is caused by problems with the correlation method at this particular wavelength rather than by the spectroradiometer.

After the data was wavelength corrected using the shift-function described above, the wavelength accuracy was tested again with the Fraunhofer method. The result is shown in Figure 5.3.9. At 320 nm, the wavelength shift for noontime measurements is smaller than ± 0.075 nm throughout the season. The actual wavelength uncertainty may be a little larger because of wavelength fluctuations during the day of about ± 0.02 nm and possible systematic errors of the Fraunhofer correlation method (see Section 3). The shifts for other wavelengths in the UV have a very similar pattern to the shift at 320 nm presented in Figure 5.3.9.

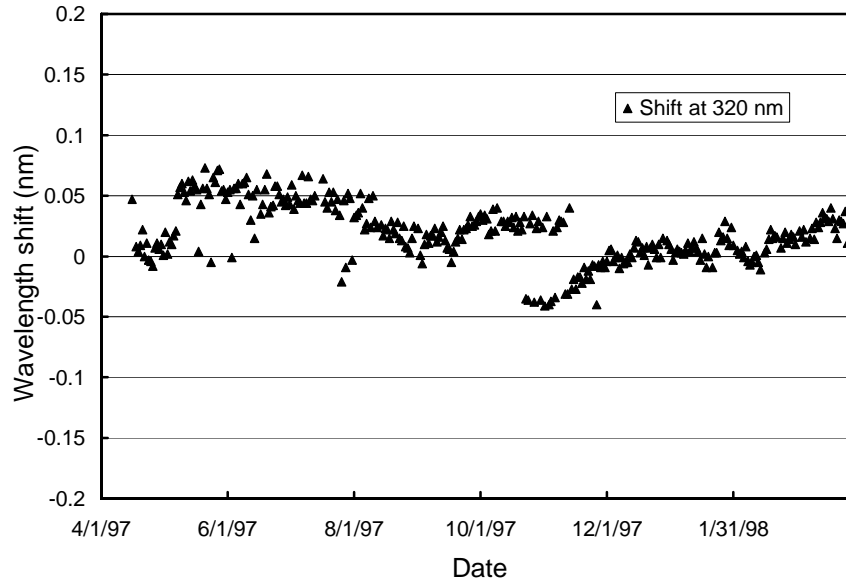


Figure 5.3.9. Check of the wavelength accuracy of the final data by means of Fraunhofer correlation. The noontime measurement has been evaluated for each day of the season. Between 10/23/97 and 11/13/97 the shift fluctuates randomly between about -0.04 nm and +0.04 nm. The reason is unknown.

Although the data from the external mercury scans do not have a direct influence on the data products, they are an important part of instrument characterization. Figure 5.3.10 illustrates the difference between internal and external Mercury scans collected during both site visits. External scans have a bandwidth of about 1.0 nm FWHM, whereas the bandwidth of the internal scan is only 0.72 nm. In addition, the peak of external scans is shifted towards longer wavelengths compared to the peak of internal scans. Since external scans have the same light path as solar measurements, they more realistically represent the bandpass of the monochromator. The difference in the center wavelength of both scan types is consistent with the wavelength bias found by the Fraunhofer correlation method of about 0.11 nm. The scans at the start and end of the season are very consistent, as can be seen from Figure 5.3.10.

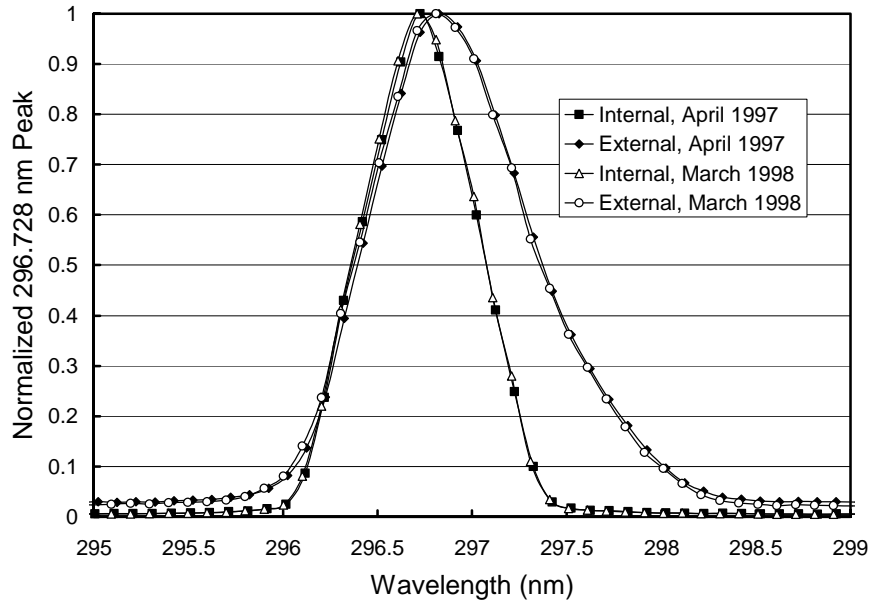


Figure 5.3.10. The 296.73 Mercury line as registered by the PMT from external and internal sources. For this plot, the wavelength calibration is based on the internal scans and it was assumed that the wavelength registration of the monochromator did not shift between internal and external scans, which were close in time.

5.3.3.2. Responsivity Stability

The stability of the spectroradiometer's responsivity over time is monitored with the internal response lamp. However, this lamp is also subject to change and it is therefore important to also assess the stability of this lamp. In some instances, however, it may not be clear whether observed drifts are attributable to the response lamp or to the spectroradiometer. In these cases, the biweekly calibrations with 200-Watt irradiance standard lamps provide a way to determine the ultimate stability of the whole system. In the 1997/98 Palmer season, the response lamp showed a considerable drift during the first three months, as explained below. With the help of the external calibrations, however, it was possible to demonstrate that the spectroradiometer itself was stable to within $\pm 1\%$. Also in the period, which was affected by the response lamp drift, the lamp provided useful information on short-term instrument stability in the gaps between consecutive external calibrations.

Instrument and response lamp stability are primarily assessed using four parameters:

- Total Scene Irradiance (TSI) UV-A, filtered-photodiode sensor measurements
- Photomultiplier Tube (PMT) current at several wavelengths
- Current supplied to the lamp
- Calibrations with 200-W standards

Note that the TSI sensor is completely independent from possible monochromator and PMT drifts, whereas the PMT current is affected by all system parts, including response lamp, monochromator, and PMT, and is also sensitive to temperature changes and high voltage applied. PMT current therefore also provides valuable insight into possible drifts of these components.

Figure 5.3.11 shows the PMT current at 300 and 400 nm and the TSI behavior during the whole 1997/98 Palmer season. The season is broken into three periods. All data are normalized to the averages of the individual system parameters of Period 2. As can be seen from the plot, Period 1 is affected by an approximately 10% drift indicating that the response lamp exhibited an abnormally high initial drift. The variations in Period 2 and 3 variations are below $\pm 2\%$. The change in PMT current closely resembles the

change in TSI signal, suggesting that most of the drift is caused by the response lamp rather than the spectroradiometer. Figure 5.3.12 shows a close-up of Period 3. Here all data are normalized to the average in this period. All three system parameters decreased by 2% in this period.

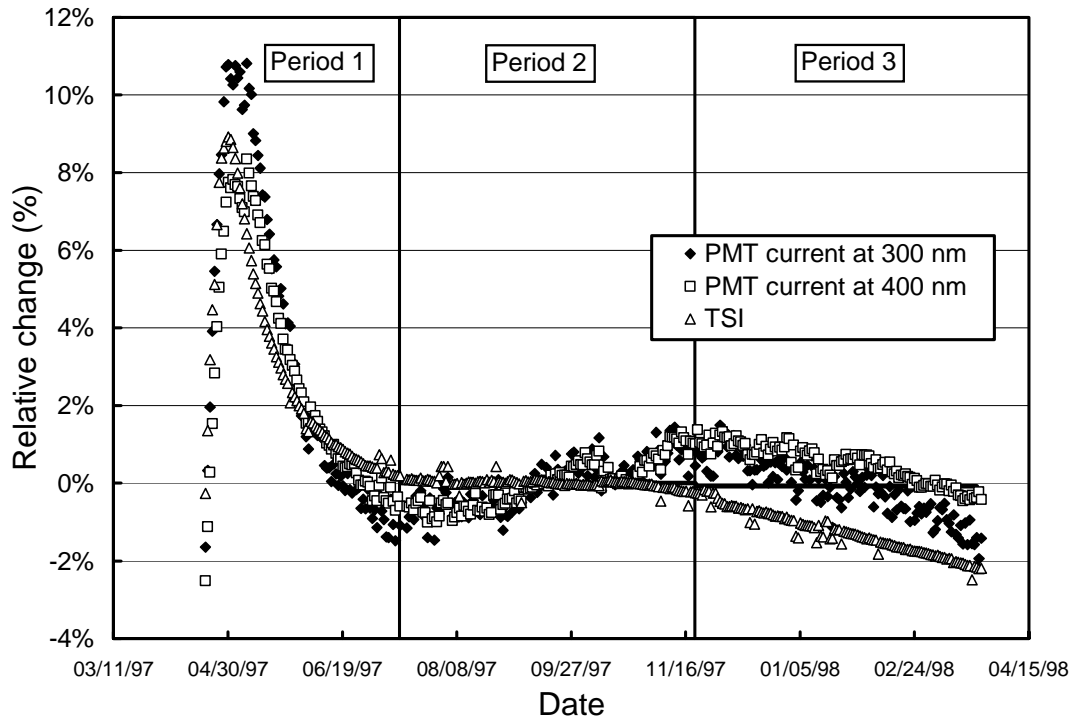


Figure 5.3.11. Time-series of PMT current at 300 and 400 nm and TSI signal during measurements of the response lamp during the Palmer 1997/98 season. The data is normalized to the average of Period 2.

For Periods 2 and 3, the system was calibrated in the usual fashion, i.e., a “mean irradiance” of the response lamp was determined based on the calibrations with the 200-Watt standards, which were carried out in each respective period. From the daily response lamp scans and these mean-irradiances the responsivity of the system for each day was then calculated (see Section 3 for details). Due to the drift of the response lamp this approach could not be applied to Period 1. We used instead the same mean-irradiance in Period 1 that was applied in Period 2. Similarly, the response scans in Period 1 were not used for the determination of system responsivity in this period but were replaced by carefully selected scans response scans from Period 2. Thus the spectroradiometer was “led to believe” that it was calibrated with a stable response lamp. This procedure leads only to a correct calibration of the spectroradiometer if the system’s responsivity does not change between Period 1 and 2. This was checked by thoroughly evaluating the scans of the 200-Watt standards. For a stable system, it can be expected that the PMT net current at a specific wavelength is the same for all calibration events with the same 200-Watt lamp. Figure 5.3.13 and Figure 5.3.14 show that this is really the case for Periods 1 and 2 of the Palmer season. There is no significant drift between the calibrations during site visit day 4/16/97, which precedes Period 1, and day 8/29/97, which is part of Period 2.

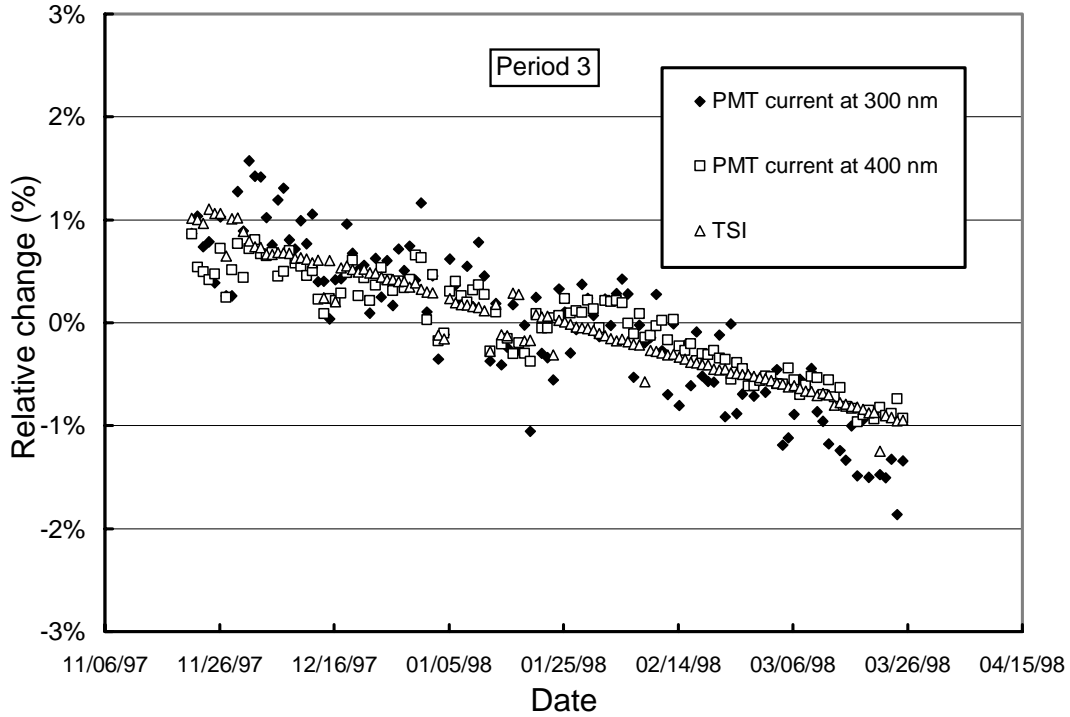


Figure 5.3.12. Time-series of PMT current at 300 and 400 nm and TSI signal during measurements of the response lamp in Period 3 (11/21/97-3/25/98) of the Palmer 1997/98 season. The data are normalized to the average in this period.

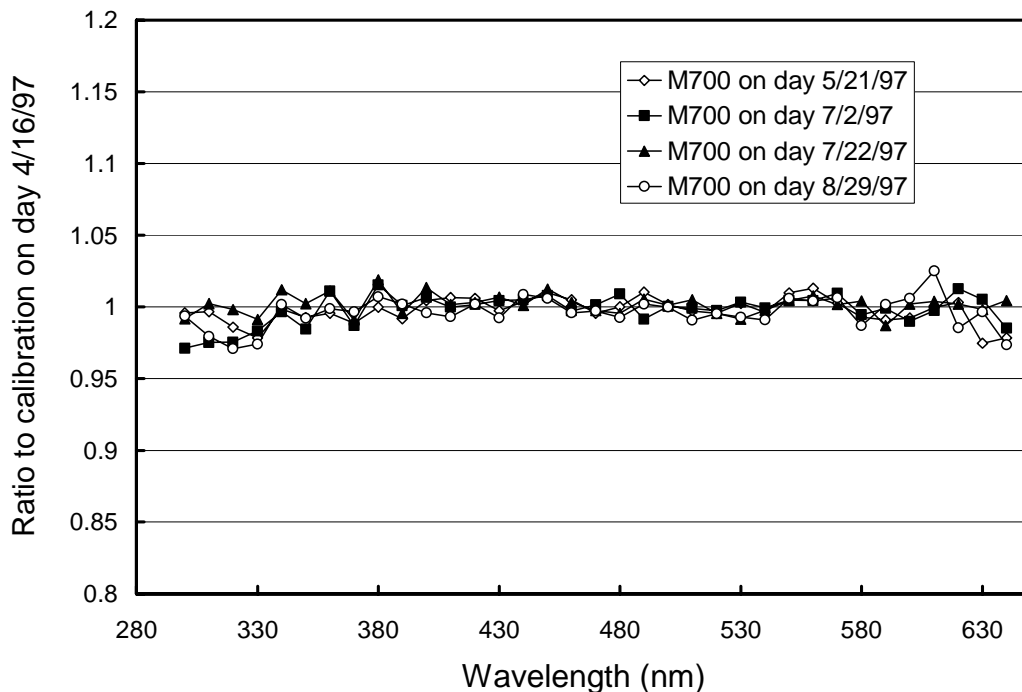


Figure 5.3.13. Comparison of PMT net current when measuring lamp M-700 during Periods 1 and 2. All data are ratioed against the measurement on day 4/16/97, the calibration day of the site visit preceding Period 1. There is no significant drift in the lamp scans; the standard deviation calculated from all points is 1%.

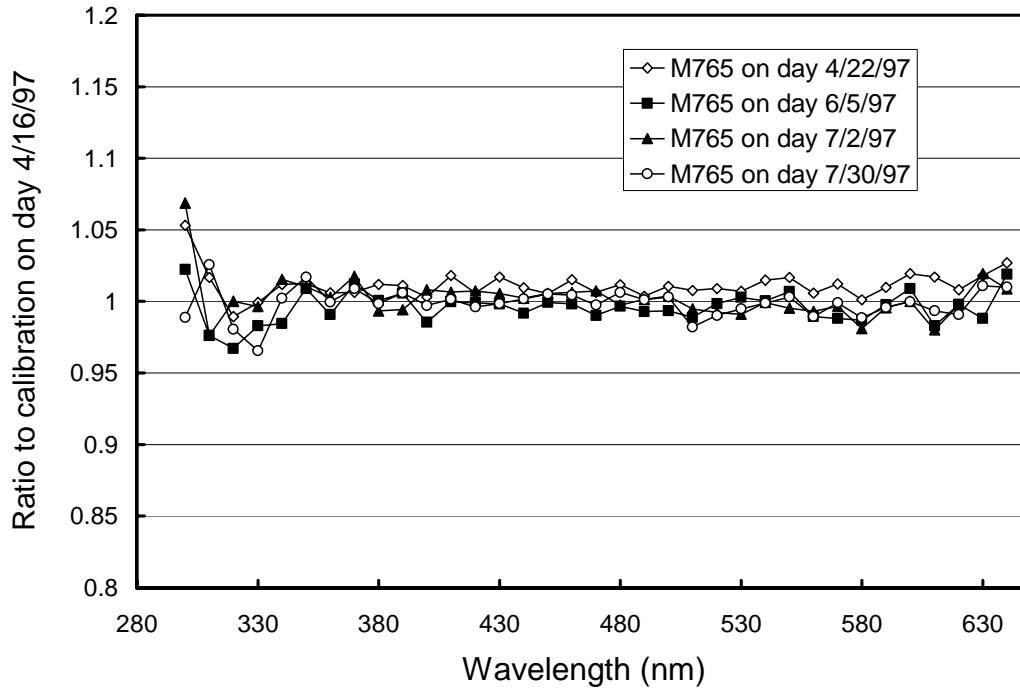


Figure 5.3.14. Same as Figure 5.4.13 but for lamp M-765. No significant lamp drift is found for this lamp either; the standard deviation calculated from all points is 1.3%. The somewhat larger scatter below 330 nm is likely caused by noise rather than instrument drift.

The “mean-irradiance” assigned to the response lamp in Period 2 was calculated from twelve 200-Watt lamp calibrations carried out in this period. From each of these calibrations, irradiance values for the response lamp were calculated and the mean-irradiance was derived by averaging over the individual calibration functions. (For more details about the definition of the “mean-irradiance”, see Section 3). The ratio of the standard deviation and average mean-irradiance, both calculated from the 12 calibration functions, is a useful tool to estimate the variability of the calibrations in this period. As shown Figure 5.3.15, the standard deviation is usually about 1% of the average and increases slightly towards shorter wavelengths. Thus the calibrations in Period 2 are consistent at the $\pm 1\%$ ($\pm 1\sigma$) level. The same procedure was also applied to Period 3 and the standard-deviation-to-average ratio for this period is also shown in Figure 5.3.15.

Figure 5.3.16 shows the mean-irradiance applied in Period 3 divided by the respective irradiance of Period 2. This ratio expresses the difference in the system’s responsivity between the two periods. Between 309 and 600 nm the ratio is to within $\pm 1\%$. At 290 nm the difference is 2.2%.

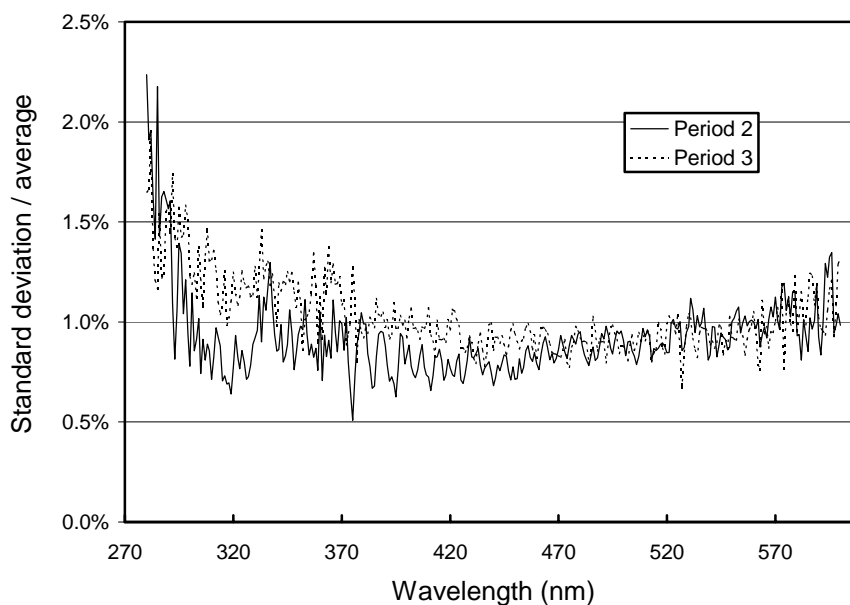


Figure 5.3.15. Ratio of standard deviation and average calculated from the absolute calibration scans of Periods 2 and 3.

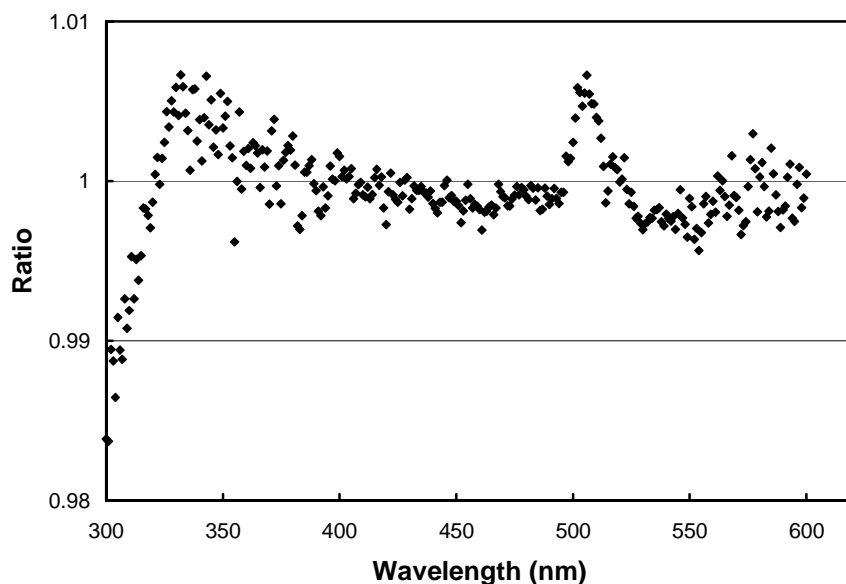


Figure 5.3.16. Ratio (Period 3 / Period 2) of the response lamp's "mean irradiance."

5.3.3.3. Lamp Intercomparison and Calibration Events

In the 1997/98 season the new standard 200W007, which was calibrated by Optronic Laboratories in 1996, was first deployed as a Palmer site standard. At both sites visits encompassing the Palmer 1997/98 season, this lamp was compared with the other two site standards, M-765 and M-700, and the BSI traveling standard M-874 to evaluate the level of consistency between the calibration values of all four lamps. Figure 5.3.17 and Figure 5.3.18 show the results of the comparison for the season starting and closing site visits, respectively. The comparison at the season-start is affected by the drifting response lamp, which partially explains the larger discrepancy between the lamps compared to the season-end comparison. Figure 5.3.17 has therefore to be judged with caution. The general pattern is the same, however, for both figures. The curve for M-874 is high, the ratio for 200W007 is low, and lamps M-700 and M-765 lie approximately in the middle. In Figure 5.3.18, all lamps agree approximately on the $\pm 2\%$ level.

Optronic Laboratories established the calibration values of the traveling standard M-874 in 1998, about half a year after the Palmer site visit. An Optronic Laboratories calibration from 1995 exists for this lamp, which deviates by about 2% from the 1998 calibration values. If the 1995 values had been used in Figure 5.3.18 the curves for lamps M-874 and 200W007 would be closer together.

Optronic Laboratories calibrated lamp M-765 in 1992. Possible drifts of this lamp between 1992 and the 1997/98 season may account for the somewhat spectrally dependent difference with the new lamp 200W007. Lamp M-700 was calibrated during a previous site visit and not by Optronic Laboratories. Comparison with this lamp must therefore be treated with caution. From the evaluation of both calibration events we conclude that the irradiance scale applied for Volume 7 Palmer data is in $\pm 2\%$ agreement with the Optronic Laboratories calibration scale from 1998, which in turn is traceable to primary NIST irradiance standards.

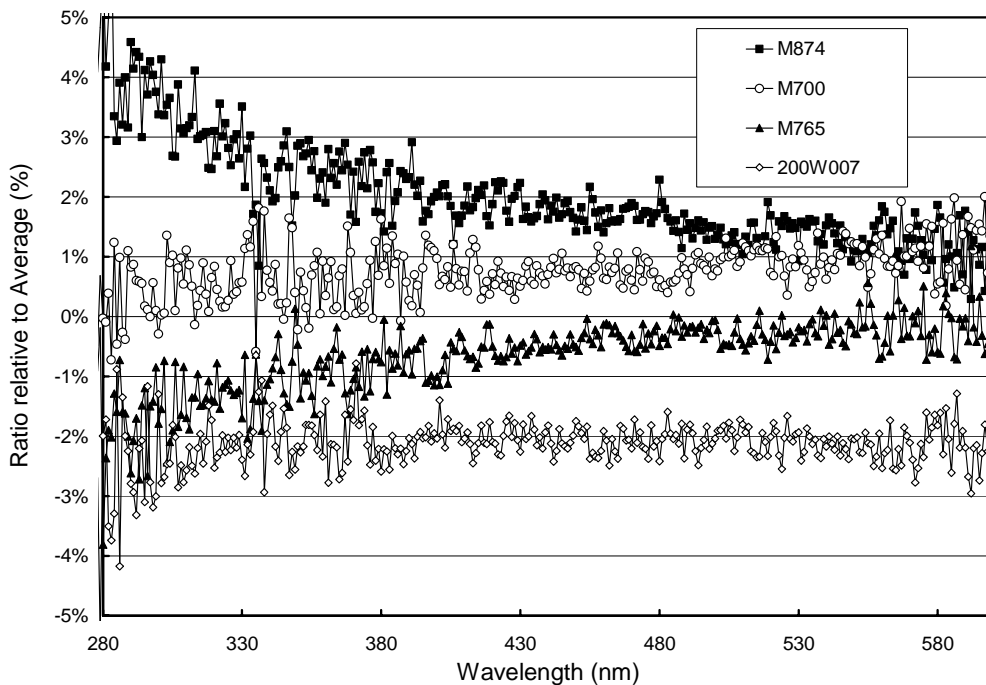


Figure 5.3.17. Comparison of Palmer lamps M-765, M-700, and 200W007 with the BSI traveling standard M-874. All measurements were performed at the start of the season on day 4/16/97.

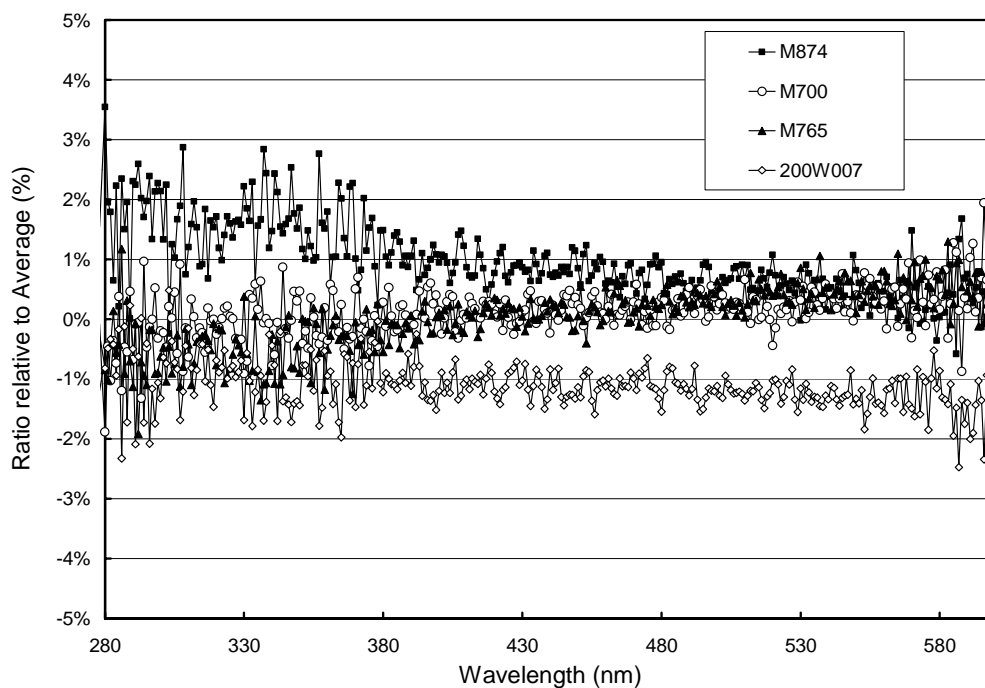


Figure 5.3.18. Comparison of Palmer lamps M-765, M-700, and 200W007 with the BSI traveling standard M-874. All measurements were performed at the end of the season on day 3/26/98.

5.3.3.4. Missing Data

A total of 17215 scans with SZA smaller than 92° were scheduled to be measured in the Palmer Volume 7 season. This is a substantial increase compared to previous seasons. This enhancement is the result of a change in the scan schedule on day 6/31/97, from 2 scans per hour to 4 scans per hour. A total of 17015 scans, 98.8% of the scans scheduled, were actually measured, and 16872 scans (98.0%) are included in Volume 7. The discrepancy of 200 scans between scheduled and measured data scans is primarily caused by other scan types, which superseded solar measurements. For example, 64 response scans and 26 wavelength scans were measured when the SZA was smaller than 92° . Since Palmer station has almost 24 hours of sunlight per day in December, a loss of data scans cannot be avoided. Most of the remaining 110 missing data scans are caused by external calibrations performed during the day.

Not all scans measured are part of Volume 7. Some scans were found to be defective and were therefore excluded from the final data set:

- 25 scans were excluded on days 7/15/97 and 7/16/97 because of problems with the wavelength calibration;
- All 32 scans performed on day 8/5/97 were found to be defective; and
- 113 scans on days 12/18/97 and 12/29/97 could not be processed because of erroneous logfile and disk write errors.

